ELSEVIER

Catalysis Today 28 (1996) 415–429

CATALYSIS TODAY

Induction of activity and deactivation of Fe, Mn-promoted sulfated zirconia catalysts

M.A. Coelho [a], W.E. Alvarez [a,1], E.C. Sikabwe [b], R.L. White [b], D.E. Resasco [a,*]

[a] *School of Chemical Engineering, University of Oklahoma, Norman, OK 73019, USA*
[b] *Department of Chemistry and Biochemistry, University of Oklahoma, Norman, OK 73019, USA*

Abstract

The isomerization of n-butane on sulfated zirconia catalysts promoted by the addition of Fe and Mn ions has been studied. The evolution of the catalytic activity of these materials as a function of time on stream exhibits a typical shape containing an induction period during which the activity increases. The induction period is followed by a rapid deactivation and then a slower deactivation. The shape of the conversion–time curves contains important information about the way these catalyst operate. Slight changes in the preparation and pretreatment of the catalysts result in changes in the overall activity and shape of the conversion–time curves. The results of this study suggest that the induction period is due to the formation and accumulation of reaction intermediates on the surface. These intermediates participate in the reaction as part of an inter-molecular mechanism. The n-butane molar fraction, the presence of olefins or hydrogen in the feed, and the reaction temperature strongly affect the induction period.

A simple mathematical model that successfully describes the behavior of the conversion–time curves has been developed. This model is consistent with the existence of two types of sites with different reactivity and stability. One type is responsible for most of the activity observed during the first few minutes on stream, but it is rapidly deactivated. This type of sites is easily deactivated by simple exposure to hydrogen, so it is consistent with an oxidized species recently proposed. The second type of sites is more resistant to deactivation.

1. Introduction

A few years ago, Hsu et al. [1,2] reported that Fe and Mn oxides were able to promote sulfated zirconia making it active for the isomerization of n-butane at temperatures as low as 35°C. Without the Fe and Mn, sulfated zirconia can isomerize n-butane, but it requires temperatures in the range of 180–200°C [3]. Subsequently, other researchers [4] confirmed this remarkable discovery and reproduced the active catalysts. The nature of this promotion, which is one of the topics of this paper, is still a matter of discussion. In fact, even the activity of unpromoted sulfated zirconia catalysts has not been fully explained and different models for the structure of the acid site have been proposed in the literature. For example, in their pioneering work Tanabe et al. [5,6] proposed a bidentate sulfate species containing a O = S = O moiety. Later, Bensitel et al. [7], based on the results of isotope exchange experiments which were not consistent with the presence of O = S = O groups but rather a single –S = O, proposed the

* Corresponding author
[1] Permanent address: INTEMA, Facultad de Ingenieria, Universidad Nacional de Mar del Plata, (7600) Mar del Plata, Argentina.

PII S0920-5861(96)00250-7

presence of tridentate SO_4 species containing a single $-S=O$ moiety. We have recently proposed our own model which also contains a single $-S=O$, but in this model each sulfur atom is surrounded by five different oxygens. In our model the Lewis acid form of the catalyst can be conceptualized as arising from the insertion of a planar SO_3 molecule into the (001) crystallographic plane of tetragonal ZrO_2. The Bronsted acid site can be obtained by the attack of a water molecule on a Zr atom Lewis acid site. On the basis of spectroscopic evidence, we have suggested that the proton associated with the S–O oxygen would more likely be responsible for Bronsted acidity than the Zr–O–H proton. There is no general consensus of how to relate the isomerization activity of sulfated zirconia to Lewis acidity [8], Bronsted acidity [9], or a combination of the two [10,11], but it is known that both types of sites are present under reaction conditions [12]. In addition, it is generally agreed that the crystalline form of zirconia plays a role in determining the surface acidity and, consequently, the catalytic activity [13]. Upon heating, zirconium hydroxide in contact with sulfur-containing species is converted into amorphous zirconium oxide that subsequently crystallizes into a tetragonal form, and, at higher temperature, this tetragonal form is converted to a monoclinic phase [14]. The temperatures corresponding to the onset of crystallization and to the formation of the monoclinic phase are higher for sulfated zirconia than for zirconium oxide [15]. The temperature at which sulfate decomposition is detected for sulfated zirconia coincides with the ZrO_2 tetragonal to monoclinic phase transition [16], suggesting that monoclinic sulfated zirconia may not be stable. In the tetragonal phase bulk, each zirconium atom is coordinated to eight different oxygens. Four Zr–O bonds are significantly shorter than the other four. The four short Zr–O bonds constitute one distorted tetrahedron and the four longer Zr–O bonds constitute another distorted tetrahedron [17]. In the absence of adsorbates, zirconium atoms at the (001) plane of tetragonal zirconium oxide are coordinated to only six different oxygens. Each zirconium atom can therefore interact with surface adsorbates through the two vacant coordination sites [18]. We have postulated that these surface coordination sites can be occupied by oxygenated sulfur species. The facts that crystallization can be retarded for sulfated zirconia and that the tetragonal phase is stabilized when sulfur-containing species is present indicate that the acid site structure is sensitive to the separation between the metal and oxygen atoms at the oxide surface. For instance, monoclinic ZrO_2 is less dense than tetragonal ZrO_2 because its unit cell is larger. The multiple interactions postulated in our model may not be possible for monoclinic ZrO_2 because the Zr–O–Zr spacing is too large. Therefore, the most active sites would be related to the tetragonal form. Recent Raman studies conducted at Northwestern University [19] suggest that the active catalysts contain the tetragonal phase and that catalyst deactivation is accompanied by a tetragonal-to-monoclinic phase transformation.

The addition of Fe and Mn promoters to sulfated zirconia further complicates the picture because they generate a low temperature activity which is not present in unpromoted sulfated zirconia. Most of the reports on Fe, Mn-promoted catalysts indicate that the isomerization activity exhibits a typical pattern when measured as a function of time on stream in the absence of added hydrogen. The initial activity is very low, but as the reaction proceeds, the conversion slowly increases, reaches a maximum, and then starts decreasing. In this contribution we have investigated the origin of this behavior which we will describe in terms of three contributions to the overall conversion–time curve: an induction period, a rapid deactivation, and a slow deactivation. We have found that the shape of this curve is a strong function of the feed composition, temperature, and catalyst history. Important information about the nature of the catalyst can be obtained from the analysis of these curves.

2. Experimental

2.1. Catalyst preparation

Most of the data reported in this study were obtained on a sample that we identify as catalyst S. For comparison, several other catalysts were prepared by introducing slight differences in the preparation method. For all the catalysts reported here we used the same $Zr(OH)_4$ precursor, which was prepared by precipitation of 0.5 M zirconium tetrachloride solution by dropwise addition of NH_4OH. The resulting $Zr(OH)_4$ had a BET surface area of 166 m^2/g, a pore volume of 0.28 cm^3/g, and an average pore size of 6.2 nm. These physical properties were measured in a Micromeritics ASAP 2010 adsorption apparatus. The samples were further characterized by thermal gravimetric analysis (TGA) coupled to a mass spectrometer. The TGA/MS system allowed us to measure weight losses and simultaneously identify the nature of the species evolved.

Catalyst S, which is the most active catalyst that we have tested so far, was prepared by co-impregnating the $Zr(OH)_4$ precursor with an aqueous solution of Fe and Mn nitrate. This solution, containing 0.12 g Fe/cm^3 and 0.017 g Mn/cm^3, was impregnated onto the previously dried $Zr(OH)_4$ precursor using a liquid/solid ratio of 0.756 cm^3 per gram of $Zr(OH)_4$. When referred to the final ZrO_2 support, these amounts represent nominal Fe and Mn loadings of about 1.7 wt.-% Fe and 0.5 wt.-% Mn, respectively. After drying for 12 h at 110°C, the solid was immersed for 2 h in a well stirred 1M $(NH_4)_2SO_4$ solution, using a liquid/solid ratio of 7.5 per gram of $Zr(OH)_4$. Following this soaking step, the solid was allowed to settle and was separated from the liquid. Without further washing, the solid was dried overnight at 110°C and then calcined at 600°C in an oven for a period of 4 h followed by a second calcination period of 12 h at the same temperature. The final analysis of the calcined sample (performed at Galbraith Lab. Inc.) indicated that the catalyst contained 1.7 wt.-% Fe, 0.07 wt.-% Mn, and 3.1 wt.-% S. The low Mn content was probably due to the loss of Mn during immersion in the ammonium sulfate solution. The BET surface area was 118 m^2/g, the pore volume was 0.29 cm^3/g, and the average pore size was 10 nm.

The other four catalysts investigated contained 1.5 wt.-% Fe, 0.5 wt.-% Mn, and 2.7 wt.-% S. In these four samples, the addition of the sulfate was done by incipient wetness impregnation with $(NH_4)_2SO_4$ solution. As indicated in Table 1, the order of adding Fe, Mn, and sulfate was varied in these samples. In two of these samples, we investigated the effect of an intermediate calcination at 400°C between the impregnation steps. Finally, the samples were calcined in static air at 600°C for 12 h. It is important to note that the final calcination

Table 1
Summary of catalyst preparation variables

Sample	Fe (wt.-%)	Mn (wt.-%)	S (wt.-%)	Order and method of addition	Intermediate calcination	Final calcination
S	1.7	0.07	3.1	Fe–Mn (imp.) S (soak)	NO	600 C, 4 h + 12 h
I-1	1.5	0.5	2.7	Fe–Mn (imp.) S (imp.)	NO	600 C, 12 h
I-2	1.5	0.5	2.7	Fe–Mn (imp.) S (imp.)	400 C, h	600 C, 12 h
I-3	1.5	0.5	2.7	S (imp.) Fe–Mn (imp.)	NO	600 C, 12 h
I-4	1.5	0.5	2.7	S (imp.) Fe–Mn (imp.)	400 C, 4 h	600 C, 12 h

needs to be done after the addition of sulfate. A sample that was calcined at 600°C for 4 h before sulfate addition exhibited a drastic drop in surface area (53 m^2/g) and a very low catalytic activity.

2.2. n-Butane isomerization activity measurements

n-Butane isomerization was studied in a flow reactor. In each run, 100–400 mg of catalyst was placed in a stainless steel downward-flow packed bed reactor. The reaction system allows for precise control of flow rates and temperature. The feed was a mixture of n-butane (99.9% purity from Matheson) and He (99.999% purity from Sooner Air Gas). Prior to each reaction run, the catalysts were activated in situ by flowing dry air at 600°C for 2 h. They were cooled under air to the reaction temperature, flushed in a He stream, and finally exposed to the feed mixture. The n-butane flow rate was kept constant at 10.92 cm^3/min for all runs. To vary the n-butane molar fraction, the He flow was varied. The reaction products were analyzed by a HP-5890 gas chromatograph, controlled by ChemStation software and equipped with a 50 m KCl/Al_2O_3 capillary column and a flame ionization detector.

Since n-butane isomerization on Fe, Mn-promoted sulfated zirconia catalysts exhibited a strong time dependence, particular attention had to be paid to avoid introducing extra variables that could modify the conversion–time curve. For example, we took special care in making sure that the feed composition attained its steady state before starting the activity determinations. Otherwise, changes in the feed may have resulted in conversion changes that were not related to the type of activity variations that we wanted to investigate. We monitored the total carbon signal in the FID to determine the n-C_4 molar fraction in the feed. By having the feed pre-mixed through a by-pass line and minimizing the length of the line between the reactor and the sampling valve, a constant molar fraction was obtained in less than 1 min. In this way we were able to monitor the variation of conversion from the very beginning and take data points every minute. When doing these measurements we lost the information on the by-products (C3 and C5 hydrocarbons). In some selected runs the concentration of C3 and C5 in the products was measured. In all cases, the selectivity towards isobutane was higher than 85%, and in most cases, it was higher than 90%.

3. Results and discussion

3.1. Activity of several Fe, Mn-promoted sulfated zirconia catalysts

The n-butane isomerization rates obtained at 100°C on the four catalysts investigated are summarized in Table 2 and compared to rates reported in the literature for similar Fe, Mn-promoted sulfated zirconia catalysts. All the rates were calculated from the maximum conversion values. To compare data obtained at different temperatures we extrapolated all the data to 60°C using an activation energy value of 11.4 kcal/mol, as reported in Ref. [33].

A strong effect of preparation variables and thermal treatments is clearly evident. Catalyst S, prepared by soaking the Fe, Mn-impregnated sample in the ammonium sulfate solution was the most active catalyst. Among the I series, prepared by impregnation, the most active sample was I-2 for which the Fe and Mn was added first and an intermediate calcination at 400°C was employed before the addition of sulfate. It is shown that, depending on the preparation the activity of the Fe, Mn- promoted catalysts can vary by more than one order of magnitude. However, it must be noted that even the least active of the promoted catalysts is 15 times more active than the unpromoted sulfated zirconia.

As summarized in Table 3, an interesting result was obtained on sample S when it was pretreated by heating in flowing air at 600°C for

Table 2
Comparison of n-butane isomerization rates on different Fe,Mn-promoted sulfated zirconia catalysts

Sample	Temperature (°C)	Rate at indicated temperature (moles/g cat s)	Rate extrapolated to 60°C [a] (moles/g cat s)	Ref.
S	90	7.9×10^{-6}	2.0×10^{-6}	this work
I-1	100	4.1×10^{-7}	6.4×10^{-8}	this work
I-2	100	2.0×10^{-6}	3.2×10^{-7}	this work
I-3	100	6.1×10^{-7}	9.6×10^{-8}	this work
I-4	100	1.6×10^{-6}	2.6×10^{-7}	this work
SO_4/ZrO_2	calc. [b]	calc.	4.5×10^{-9}	[33]
FMSZ	60	9.73×10^{-7}	9.73×10^{-7}	[23]
FMSZ	calc.	calc.	2.4×10^{-6}	[33]
FMSZ	37	5.5×10^{-7}	2.0×10^{-6}	[25]
FMSZ	60	4.2×10^{-7}	4.2×10^{-7}	[26]

[a] E_a used for extrapolation = 11.4 kcal/mol, as reported in [33].
[b] Calc. = calculated from kinetic parameters reported in [33].

2 h and then switched to He flow and held at 600°C for 2 h instead of cooling in air as for the rest of the runs. In this case, the activity dropped by several orders of magnitude and it was not recovered by subsequent treatments in air at 600°C. This drastic activity loss may be due to the loss of sulfate from the catalyst surface. Fig. 1 shows the result of a TGA/MS experiment conducted on catalyst S under He flow. Depending on the preparation, the SO_2 evolution may consist of a broad single peak [34] or a series of peaks, as in the case shown in Fig. 1. It is important to note that, in all cases, the weight loss profile corresponded well with the SO_2 evolution. Both profiles indicate that the maximum sulfate loss occurred at about 670°C. The loss at 600°C was not negligible and therefore during the 2 h treatment at this temperature a significant loss of sulfate may have occurred. Other catalyst alterations, such as an irreversible reduction of iron species or sulfate groups, may also occur during the high temperature treatment in He and may result in severe deactivation. These results indicate that, after the pretreatment at 600°C, the catalyst should be cooled down to the reaction temperature under air instead of He to avoid a premature deactivation.

Table 3
Effect of thermal pretreatments on catalytic activity

In-situ pretreatment	Maximum conversion (%) [a]
(1) = air, 600°C, 2 h	36
(2) = (1) + He, 600°C, 2 h	0.6
(3) = (2) + air, 600°C, 2 h	1.5
(4) = (2) + air, 650°C, 12 h	2.7

[a] Reaction conditions: 100°C, molar fraction $y(n\text{-}C_4) = 0.35$, n-butane flow rate = 10.92 cm^3/min, 0.4 g catalyst (sample S).

3.2. Effect of varying the molar fraction of n-C_4 in the feed

As shown in Fig. 2 for the case of catalyst S, the conversion–time curve obtained at 100°C is

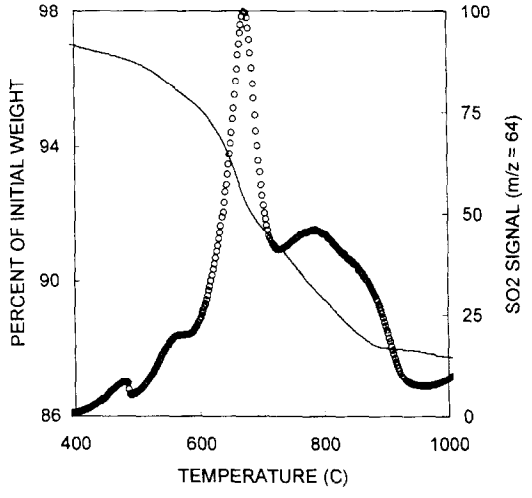

Fig. 1. TGA/MS of a fresh Fe, $Mn/SO_4/ZrO_2$ catalyst (sample S) under He flow. The solid line represents the weight loss profile (%). The symbols (○) represent the SO_2 signal ($m/z = 64$) detected in the mass spectrometer.

a strong function of the molar fraction of n-butane. The induction rate greatly accelerates when the molar fraction of n-butane increases. Similarly, the position of the maximum shifts to shorter times as the molar fraction increases. As a result, at high molar fractions the induction period may not be observed. This may explain the fact that some authors have reported the induction period [2,25,26] whereas others have not [33].

Adeeva et al. [20] have recently proposed an inter-molecular mechanism for the isomerization of n-butane on Fe, Mn-promoted sulfated zirconia involving the participation of butenes. This mechanism, first proposed by Guisnet [21,22] for H-mordenite catalysts, consists of a series of steps which include the formation of a C_4^+ carbenium ion and a butene molecule which undergo oligomerization and form a surface C_8^+ ion. This C_8^+ ion can subsequently isomerize more easily than C_4^+. A β-scission can break C_8^+ apart producing an isobutane molecule and a C_4^+ carbenium ion.

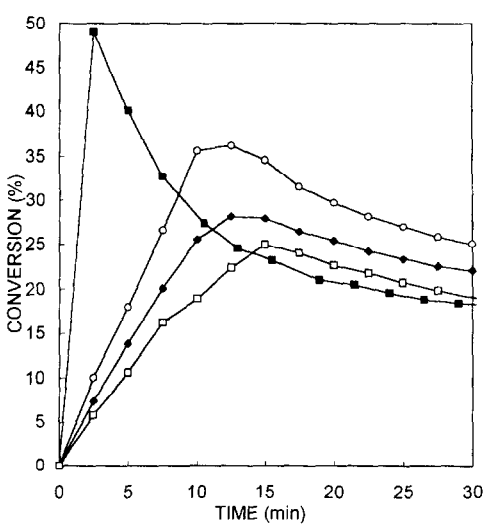

Fig. 2. Conversion–time curves at different n-butane molar fractions. n-Butane conversion to isobutane as a function of time on stream over 0.4 g of Fe, $Mn/SO_4/ZrO_2$ catalyst (sample S) at 100°C, at constant flow rate of n-butane of 10.92 cm^3/min, and at the following n-butane molar fractions $y(n\text{-}C_4)$: 0.14 (□); 0.26 (◆); 0.35 (○); 0.47 (■).

The overall mechanism can be represented by the following reaction scheme [21]:

1. C_4-carbenium ion formation on the acid site:

$$n\text{-}C_4H_{10} + H^+ \rightarrow C_4H_9^+ + H_2$$

2. butene formation (either on the acid site or the transition metal sites)

$$C_4H_9^+ \rightarrow C_4H_8 + H^+$$

3. C_8-carbenium ion formation via oligomerization

$$C_4H_8 + C_4H_9^+ \rightarrow C_8H_{17}^+$$

4. rearrangement of the C_8-carbenium ion to form tertiary carbenium ions.
5. β-scission of the rearranged ion

$$C_8H_{17}^+ \rightarrow C_4H_8 + t\text{-}C_4H_9^+$$

6. desorption of isobutane after hydride transfer from n-butane

$$t\text{-}C_4H_9^+ + n\text{-}C_4H_{10} \rightarrow i\text{-}C_4H_{10} + C_4H_9^+$$

In support of this inter-molecular mechanism Adeeva et al. [20] conducted isotopic labeling experiments using doubly labeled ^{13}C butane and observed a binomial distribution of ^{13}C atoms in the products rather than keeping two ^{13}C atoms in the products as would be expected for an intra-molecular mechanism. The kinetics study of Zarkalis et al. [23] on Fe, Mn-promoted catalysts is also consistent with an inter-molecular mechanism. They have found rate equations and by-products similar to those reported by Guisnet for the H-mordenite catalysts. This hypothesis has now been extended to Pt-promoted sulfated zirconia catalysts. Liu et al. [24] observed that the presence of 33 ppm butene in the feed caused a significant increase in the activity of a $Pt/SO_4/ZrO_2$ catalyst. At the same time, an increase in the concentration of H_2 in the feed caused a drop in rate (the kinetic order in H_2 was -1.1). This drop was reversed when the hydrogen concentration decreased. This result further supports the hypothesis that olefins play an important role in the reaction mechanism. At the same time, FTIR, NMR, and EXAFS characterizations of the Fe, Mn-promoted

catalysts [25,26] have found no evidence to justify the earlier proposal of acid strength enhancement [27].

In agreement with these ideas, we have recently proposed [28] that the role of the Fe and Mn species is to increase the concentration of olefins on the surface. However, if these catalysts are strong acids, it could be argued that olefins could not exist as such on the catalyst surface but rapidly form a C_4-carbenium ion or, as suggested above, a C_8-carbenium ion. We are working in identifying the nature of the species accumulating on the surface. At this point, we can only propose that the observed induction period is due to a slow accumulation of reaction intermediates on the surface. The results shown in Fig. 2 are consistent with this hypothesis. It would be expected that, as the n-butane concentration increases, the rate of surface species accumulation should increase, shortening the induction period as demonstrated in Fig. 2.

3.3. Effect of adding 1-butene to the feed

To further test this hypothesis, we have investigated the consequences of adding a fixed amount of butene to the feed at different times. If, as proposed above, the induction period is due to the build-up of reaction intermediates on the surface, the initial activity could be greatly enhanced by addition of butenes, since they are proposed to be some of the intermediates participating in the mechanism. In fact, as depicted in Fig. 3, the addition of 15 μl of 1-butene had a strong effect on the activity pattern when it was injected before the reaction started. In this case, the induction period was significantly shortened and the activity rapidly increased. However, the effect was not as dramatic when it was injected a few minutes after the reaction had started. We can explain this behavior in terms of the mechanism described above. When the injection was done at time zero, the surface was initially free of surface species. The sudden injection of 1-butene resulted in a rapid increase in the concentration of these species on the surface and an increase in activity. By contrast, when the injection was done after 15 min., the surface was already covered by the reaction intermediates and the rapid increase of butene concentration in the gas phase did not represent a big change in the surface concentration. Consequently, there was no significant increase in activity.

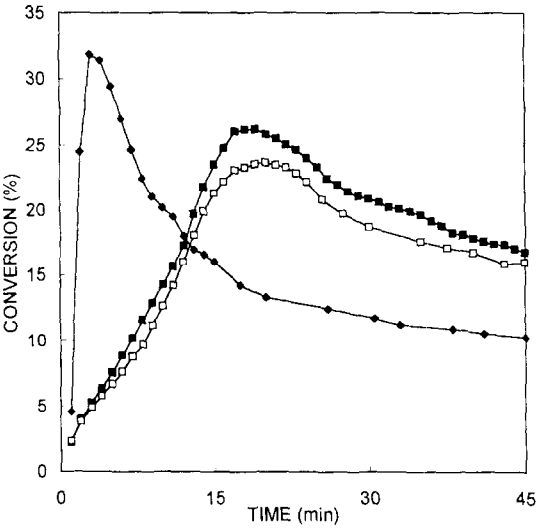

Fig. 3. Modification of conversion–time curve for Fe, Mn-promoted catalyst by injections of 1-butene in the feed. (◆) 15 μl injected before starting the run; (■) 15 μl injected after 15 min on stream; (□) no injection. Reaction conditions: $T = 100°C$; $y(n\text{-}C_4) = 0.35$; 0.4 g Fe, $Mn/SO_4/ZrO_2$ catalyst (sample S).

It has been proposed that the role of the transition metal species is to generate olefins [20]. We have repeated the experiments described above using an unpromoted sulfated zirconia to test whether the addition of olefins to bare sulfated zirconia resulted in activity levels close to those observed on Fe, Mn-promoted catalysts. However, as shown in Fig. 4, the observed enhancement in the activity of the unpromoted sulfated zirconia by injection of 1-butene was not enough to get even close to that of the promoted catalysts. Although the activity increased by a factor of 3 to 4 by addition of 1-butene, the conversion level was significantly less than 1%. By contrast, the conversion on the Fe, Mn-promoted catalyst, without the addition of 1-butene, was about 25% at the maximum, and close to 7% after 45 min on

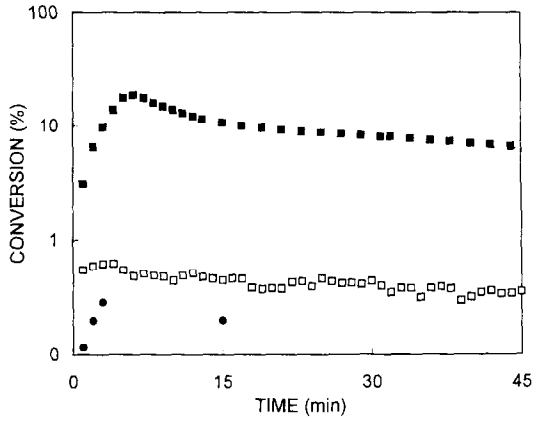

Fig. 4. Semi-logarithmic conversion–time curve for unpromoted sulfated zirconia after injection of 1-butene in the feed. Comparison with the conversion–time curve obtained for Fe, Mn-promoted catalyst. (□) SO_4/ZrO_2 catalyst, 15 μl injected before starting the run; (●) SO_4/ZrO_2 catalyst, no injections; (■) Fe, $Mn/SO_4/ZrO_2$ catalyst (sample S), no injections. Reaction conditions: $T = 100°C$, 0.4 g catalyst, n-butane flow rate = 10.92 cm^3/min, $y(n\text{-}C_4) = 0.35$; diluent He.

stream. One explanation for this difference is that the addition of olefins from the gas phase is not analogous to the surface production of olefins by the transition metal compounds. Butenes are very reactive on acid catalysts and may oligomerize forming coke if present in relatively high concentrations. A second explanation for the low increase in activity observed on the unpromoted sulfated zirconia after addition of butene is that the Fe species are needed to interact with the olefins before they react with the C_4 carbenium ions to form the C_8^+ intermediate.

3.4. Effect of adding hydrogen to the feed

We have also studied the effect of adding a small amount of hydrogen to the feed while keeping the molar fraction of n-butane constant. As illustrated in Fig. 5, the addition of hydrogen in a H_2/He ratio of 0.1 resulted in a significant reduction in the activity level and a much slower induction. When the amount of H_2 was increased to a H_2/He ratio of 0.2 the effect was more pronounced. This is another indication that the surface concentration of olefins plays an important role in the reaction. It would be expected that as the hydrogen concentration increased the olefin coverage should decrease, causing a decline in both the induction and the overall rates. Recently, Sachtler et al. [29] have found very suggestive differences in the H_2 dependence of the isomerization of n-butane and n-pentane over $Pt/SO_4/ZrO_2$ catalysts. While the n-butane isomerization exhibited a negative order in H_2, in good agreement with our results, the n-pentane isomerization did not depend on H_2 concentration. The authors explained this difference by considering that the n-butane isomerization requires an inter-molecular process while n-pentane isomerization can proceed by an intra-molecular mechanism. The difference between the two mechanisms is due to the activation of a common intermediate, a protonated cyclopropane ring [30]. The opening of this intermediate involves a thermodynamically unfavorable primary carbenium ion in the case of n-butane, but it can proceed through a secondary carbenium ion in the case of n-pentane.

In addition to the overall decline in activity, there is an interesting feature that appears when hydrogen is incorporated in the feed. As shown in Fig. 5, the curves corresponding to the runs

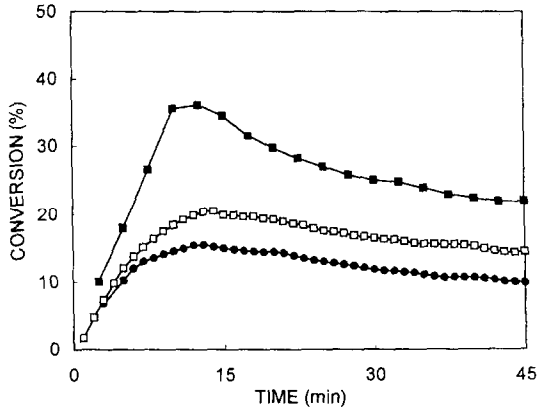

Fig. 5. Modification of activity pattern by addition of hydrogen to the feed on an Fe, $Mn/SO_4/ZrO_2$ catalyst (sample S). Reaction conditions: $T = 100°C$, 0.4 g catalyst, n-butane flow rate = 10.92 cm^3/min, $y(n\text{-}C_4) = 0.35$; diluent He. (■) no H_2 added; (□) H_2 added at a ratio $H_2/He = 0.1$; (●) H_2 added at a ratio $H_2/He = 0.2$.

conducted in the presence of hydrogen do not contain the sharp activity maximum observed for the run conducted in the absence of H_2. As discussed below, the presence of hydrogen not only affects the concentration of olefins on the surface but may irreversibly alter the state of the catalyst.

3.5. Effect of varying the reaction temperature

The catalytic behavior of Fe, Mn-promoted catalysts is a very strong function of the reaction temperature. In fact, it has been shown that, for cracking reactions, the promotion of the added transition metal species is no longer evident at high temperatures [31,32]. We studied the evolution of the activity of catalyst S at different temperatures and observed that the conversion–time curves greatly changed as the temperature was varied. For example, Fig. 6 indicates that the slope of the induction period increased rapidly when the temperature increased. The fact that the rate of induction increases with temperature would indicate that the induction is associated with a reaction step.

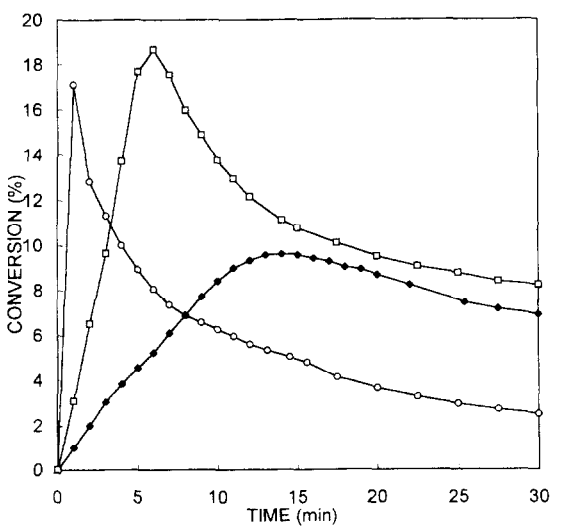

Fig. 6. Conversion–time curves at different temperatures over a Fe, $Mn/SO_4/ZrO_2$ catalyst (sample S). Flow rates: 10.92 cm^3/min n-butane; 0.1 g of catalyst; 20.6 cm^3/min He. Molar fraction $y(n\text{-}C_4) = 0.35$. Reaction temperatures: (♦) 90°C; (□) 110°C; (○) 150°C.

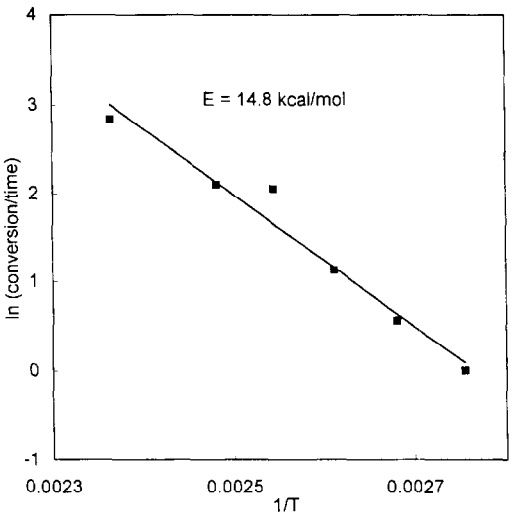

Fig. 7. Arrhenius plot for the initial slopes of the induction periods in the conversion–time curves measured at different temperatures. The E value obtained from the slope would represent the activation energy of the induction process.

The reaction temperature not only affected the induction period, but also the rate of deactivation. As a consequence, the activity maximum appeared at different times as the temperature changed. Other authors have reported the appearance of activity maxima at later times than those reported here [4,25,26]. For example, working at 30°C and at space velocities much lower than those used in this work, Tabora and Davis [25] found the activity maximum at about 40 min on stream. From the trend shown in Fig. 6, it becomes clear that such long induction periods were due to the low reaction temperatures used in those studies.

Activation energies have been previously calculated using the conversion extrapolated to zero time [33], or the conversion at the maximum [23]. However, neither of these methods resulted in a straight line Arrhenius plot for the temperature range investigated in this work. We were able to calculate the activation energy for the induction period by measuring the initial slopes in the conversion-time curves at different temperatures. From the Arrhenius plot shown in Fig. 7, an activation energy of 14.8 kcal/mol was obtained. It must be noted that this activa-

tion energy does not correspond to the overall rate but for the process responsible for the activity induction, which according to our hypothesis, would be the accumulation of surface species.

3.6. Catalyst deactivation and regeneration

Several activation/deactivation experiments were conducted at 100°C on catalyst S to further investigate the nature of the remarkable catalytic properties of this material. Fig. 8 shows a comparison of the conversion–time curves obtained after different pretreatments at a n-C_4 flow rate of 10.92 cm^3/min and a molar fraction of 0.35. The first run on the sample pretreated under a dry air flow at 600°C exhibited the characteristic induction period during which the conversion reached about 35%. This induction period was followed by an initially rapid deactivation that became much slower after a few minutes.

After the first 45-minute run, the catalyst was treated in air at 300°C for 30 min. The subsequent activity curve (not shown) was clearly different from the first one. Two aspects of this conversion–time curve are important to discuss. First, the initial activity was very low and a new induction occurred. This was an indication that the induction was an easily reversible process, more consistent with the build-up of adsorbates on the surface than with a structural modification of the catalyst. The second important aspect of the observed curve was that the maximum conversion was much lower than in the first run and the rapid deactivation was absent. Only the slow deactivation took place. After this second cycle, the conversion–time curve did not significantly change during the subsequent cycles. In these cycles, the same sample was first regenerated in air for 2 h at 650°C, then reacted for 12 h until the conversion dropped to less than 1%, and further regenerated in air at 650°C for 12 h. The final reaction run is shown in Fig. 8 in comparison to the first run. The conversion–time patterns of these two samples are clearly different. It appears that the initial activity burst occurred only once. The sites responsible for that burst (type II sites) deactivated rapidly and irreversibly. Subsequent regenerations seemed to reactivate the sites of slower deactivation (type I sites).

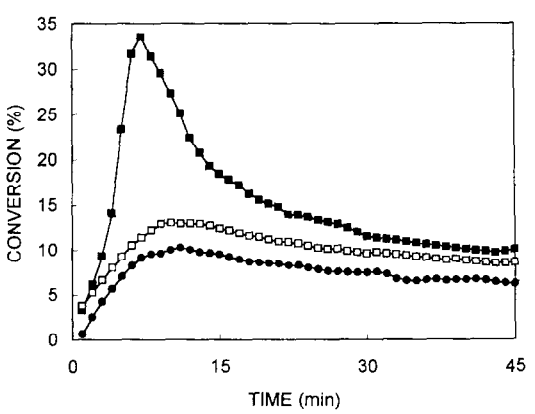

Fig. 8. Conversion–time curves over a Fe, $Mn/SO_4/ZrO_2$ catalyst (sample S) after different pretreatments. (■) First run on a fresh sample pretreated under a dry air flow at 600°C for 2 h; (□) run after three cycles of deactivation and different regenerations in air, the last one before run at 650°C in air for 12 h; (●) first run on a fresh sample pretreated under a dry air flow at 600°C for 2 h and then exposed to hydrogen prior to the reaction for 15 min at 100°C. Reaction conditions: same as those in Fig. 3.

The typical curve for a first run (fast induction and deactivation) observed for the samples pretreated in air at 600°C did not appear when the sample was pretreated in situ with air at 600°C and then exposed to hydrogen prior to the reaction for 15 min at 100°C. The conversion–time curve included in Fig. 8 is more like the second and subsequent cycles than that of a typical first run. It appears that the short exposure to H_2 at 100°C was enough to deactivate the most unstable type II sites, leaving only the type I sites. A similar behavior can be observed in Fig. 5 by comparing the conversion–time curves obtained with and without hydrogen in the feed. When H_2 was present, even at low concentrations, the fast activation/deactivation part of the curve disappeared.

These results are consistent with the presence of an oxidized species that is very active but, at the same time, deactivates very rapidly. Davis et

al. [34] have recently proposed the existence of two different iron species on the Fe, Mn-promoted catalysts. An iron 'oxy' species would be generated under high temperature treatment in air and stabilized by the surface of tetragonal zirconia. Also, under less oxidizing conditions, an iron (III) site could be formed. They have suggested that the first species would be labile but very active while the second would only be active at higher temperatures. We have no evidence to support or oppose the nature of the proposed species, but the overall idea of two types of sites with different reactivities and stabilities is certainly in good agreement with our results. Davis et al. [34] further explained the evolution of CO_2 during the benzene TPD experiments that they had previously reported in terms of the proposed species. They speculated that the iron 'oxy' species on the surface may be responsible for the decomposition and subsequent oxidation of adsorbed benzene. We have conducted similar TPD experiments using pyridine and other adsorbates and observed similar results [35]. As illustrated in Fig. 9, after the adsorption of pyridine, subsequent TPD resulted in the evolution of SO_2 and CO_2. This evolution occurs at temperatures significantly higher than those at which the n-butane isomerization is conducted, which may indicate that the oxidation of the adsorbates and deactivation of the catalyst can only occur at high temperatures. However, recent experiments conducted by the same group [34] demonstrate that reduction of the labile iron 'oxy' species may occur at room temperature when exposed to CO.

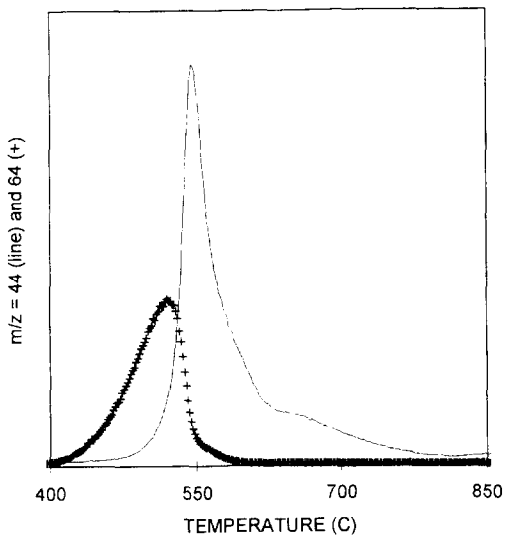

Fig. 9. Temperature programmed desorption following adsorption of pyridine on an Fe, $Mn/SO_4/ZrO_2$ catalyst (sample S). CO_2 evolution ($m/z = 44$) (————); SO_2 evolution ($m/z = 64$) (+).

3.7. Mathematical model

To describe the behavior of the two types of sites that we are postulating here, we have used a simple model that considers the time-dependent overall rate, $r(t)$, as constituted by two contributions. Each of these two rate contributions contains induction and deactivation factors. The first one, $r_1(t)$ represents the activity of the more stable type I sites, while the second, $r_2(t)$, represents the more easily deactivated type II sites (the activity burst). We have been able to fit all of our conversion–time curves by considering:

1. $r_1(t)$ as constituted by:
   - an induction factor $= A_1(1 - e^{-k_1 t})$
   - a deactivation factor $= B_1 e^{-k_{d1} t}$
2. $r_2(t)$ as constituted by:
   - an induction factor $= e^{k_{2i}t}/(A_2 + e^{k_{2i}t})$
   - a deactivation factor $= B_2 e^{-k_{d2} t}$

In Fig. 10 we illustrate the fit of one of the conversion–time curves with the mathematical model in which A_1, B_1, A_2, B_2, k_1, k_{d1}, k_2, and k_{d2} are the adjustable parameters. A non-linear regression routine was used to fit the data. As shown in Fig. 10, the model fits the data very well over the entire time range. By contrast, very poor fits resulted when we attempted to fit the conversion–time curves with only one contribution (i.e., one induction and one deactivation). The quality of the fit can be quantified in terms of R-values. The definition of R is:

$$R = 1 - \left[\Sigma(y_i - y_i')^2 / \left(\Sigma y_i^2 - (\Sigma y_i)^2/n\right)\right]$$

where y_i is a point from the model, y_i' an

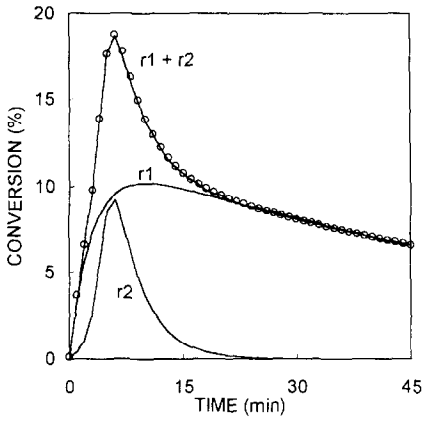

Fig. 10. Application of the mathematical model to fit experimental data obtained over sample S as a function of time. Molar fraction $y(n\text{-}C_4) = 0.35$. $T = 110°C$, 0.1 g of catalyst. (o) Experimental data; (————) model. The model includes two contributions (r_1 and r_2) to the overall rate, where

$r_1 = A_1(1 - e^{-k_1 t}) B_1 e^{-k_{d1} t}$

$r_2 = \left[e^{k_2 t}/(A_2 + e^{k_2 t})\right] B_2 e^{-k_{d2} t}$

experimental data point, and n the number of points. Accordingly, the R-value obtained for the best fit of the data shown in Fig. 10 was 0.992 when the two-contribution model was used, while it was only 0.888 and 0.881 when each of the two contributions (r_2 and r_1 respectively) were used separately.

The role of each of the two contributions, r_1 and r_2, is clearly evident in the fit. The type II sites appear to totally deactivate during the first 15 min, and after that period only the type I sites remain active.

To further test the physical validity of the model we fitted the first-run data from Fig. 8 and then independently compared each individual contribution from that fit (i.e. without changing the adjustable parameters) to experimental data that represent the activity of type I and type II sites, respectively. We plotted in Fig. 11 a the data of the first-run in the series of deactivation/regeneration experiments described in Fig. 8. We used the model to fit those data as shown in Fig. 11 a. Now we compare the $r_1(t)$ curve resulting from the fitting of the first run, to the final run in the series of deactivation/regeneration experiments. As described above, this activity would correspond to that of type I sites. Similarly, in Fig. 11 c we plotted the $r_2(t)$ curve, resulting from the fitting of the first run, together with the point-by-point difference of the first and final runs. This difference would represent the activity curve of the easily deactivated type II sites which are lost after the first run. Considering that the calculated curves in Fig. 11 b and c are not fitted to the corresponding experimental data, but rather they directly come from the fitting of the overall rate to the first run, the agreement is remarkable.

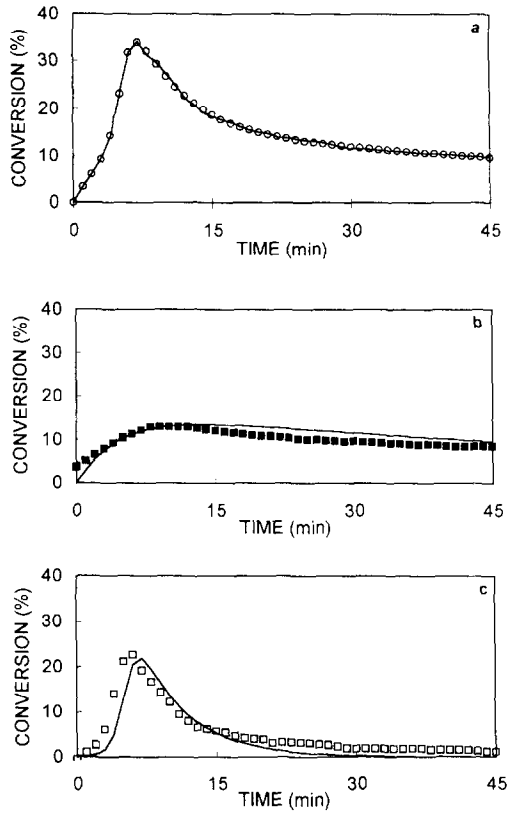

Fig. 11. (a) Application of the model (solid line) to fit the experimental conversion–time curve (○) obtained on a fresh sample of catalyst S, pretreated in air at 600°C. The contributions r_1 and r_2 to the overall rate obtained from this fit are subsequently compared to: (b) the experimental conversion–time curve obtained on the same sample after three cycles of deactivation/regeneration (■), (c) the point-by-point difference (□) between the first (a) and the final (b) runs. This difference represents the activity of the sites deactivated during the first run. Note that r_1 and r_2 directly resulted from the fitting of the experimental data shown in (a), rather than individual fits of the data shown in (b) and (c), respectively.

We have used this mathematical model to fit the conversion–time curves obtained at different temperatures. In the three cases the fit was very good with R-values of 0.99 or better. The results of the fit are illustrated in Fig. 12 for the runs at 90, 110 and 150°C. Fig. 12 a shows the variation of the contribution $r_2(t)$ as a function of temperature. The fast activation and deactivation of these 'labile' sites is clearly evident in these curves. By contrast, Fig. 12 b shows the evolution of the r_1 contribution which represents the type I sites of slower deactivation.

Fig. 13 shows the temperature dependence of the induction (k_i) and deactivation (k_d) constants obtained from the fitting. These constants show more quantitatively the overall behavior described above. The deactivation of the type II sites is faster than that of type I. In all cases, an

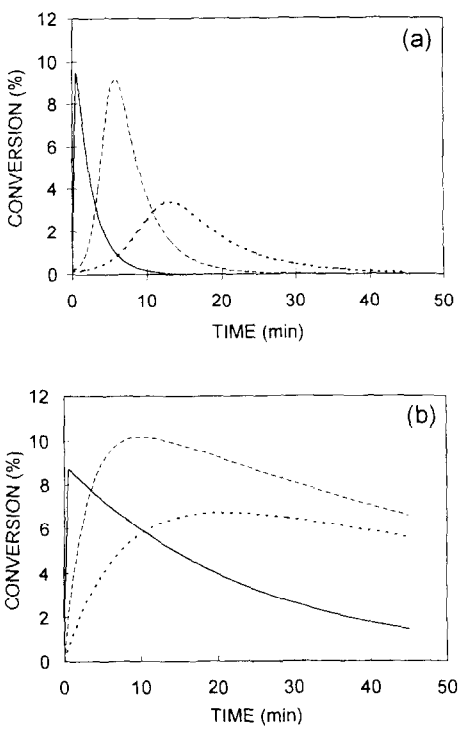

Fig. 12. Variation of the two rate contributions, r_2 (a), r_1 (b), at different temperatures, obtained by fitting the experimental data shown in Fig. 6. The quality of the fit (comparison with experimental data not shown here) was as good as that of Fig. 10 (R-values > 0.99). 90°C (dots), 110°C (dashes), 150°C (solid line).

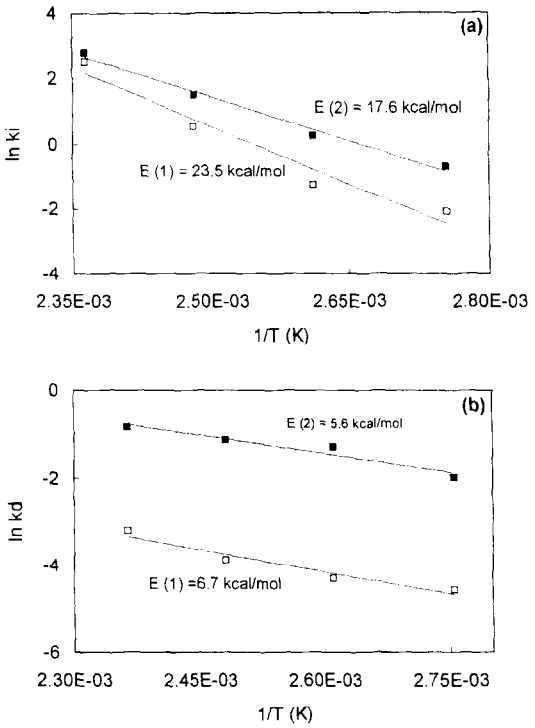

Fig. 13. Arrhenius plots for the induction (k_1 and k_2) and deactivation (k_{d1} and k_{d2}) constants for the two contributions to the overall rate, obtained from the fitting of the conversion–time curves measured at different temperatures.

Arrhenius-type behavior was observed, which further supports the physical meaning of these fitting parameters. The activation energy values obtained for the four constants are included in the figures. It is interesting to note that while the activation energies for the two induction constants were relatively high, and of the same order of the overall induction process, the activation energies for the deactivation constants were low. The former, around 15–20 kcal/mol, are typical of the surface-catalyzed reactions involved in the proposed mechanism (dehydrogenation, oligomerization, and cracking). The latter, around 5–6 kcal/mol are too low to directly represent a single surface reaction step.

4. Conclusions

- We have studied the evolution of n-butane isomerization activity as a function of time

on stream of Fe, Mn-promoted sulfated zirconia catalysts. The shape of the conversion–time curves contains important information about the mechanism of this reaction. We have observed that slight changes in the preparation and pretreatment of the catalysts result in changes in the overall activity and shape of the conversion–time curves. These curves can be described as composed by an induction period followed by a rapid deactivation and then a slower deactivation.

- We have ascribed the induction period to the formation and accumulation of reaction intermediates on the surface which participate in the reaction as part of an inter-molecular mechanism. The n-butane molar fraction, the presence of olefins or hydrogen in the feed, and the reaction temperature strongly affect the induction period. The dependence of the conversion–time curves on these variables can be taken as further evidence to support the inter-molecular mechanism.
- We have used a simple mathematical model to describe these curves. This model is consistent with the existence of two types of sites with different reactivity and stability. One type is responsible for most of the activity observed during the first few minutes on stream, but it is rapidly deactivated. This type of sites is easily deactivated by simple exposure to hydrogen, so it is consistent with an oxidized species recently proposed by Davis et al. [34]. The second type of sites is more resistant to deactivation.

Acknowledgements

This work was supported by the National Science Foundation (CTS-9403199) and the Exxon Education Foundation. We thank the University of Mar del Plata for a fellowship for one of us (WEA), as part of the international exchange program sponsored by the University of Oklahoma and the University of Mar del Plata. We thank Prof. W.M.H. Sachtler and Prof. M.E. Davis for sharing with us preprints of their respective work.

References

[1] E.J. Hollstein, J.T. Wei and C.Y. Hsu, US Pat. 4,918,041 (1990).
[2] E.J. Hollstein, J.T. Wei and C.Y. Hsu, US Pat. 4,956,519 (1990).
[3] M. Hino and K. Arata, J. Chem. Soc. Chem. Comm., (1980) 573.
[4] A. Jatia, C. Chang, J.D. MacLeod, T. Okabe and M.E. Davis, Catal. Lett., 35 (1994) 21.
[5] T. Jin, T. Yamaguchi and K. Tanabe, J. Phys. Chem., 90 (1986) 4794.
[6] T. Yamaguchi, T. Jin, T. Ishida and K. Tanabe, Mater. Chem. Phys., 17 (1987) 3.
[7] M. Bensitel, O. Saur, J.C. Lavalley and B.A. Morrow, Mater. Chem. Phys., 19 (1988) 147.
[8] R.A. Comelli, C.R. Vera and J.M. Parera, J. Catal., 151 (1994) 96.
[9] M. Nitta, H. Sakoh and K. Aomura, Appl. Catal., 10 (1984) 215.
[10] F.R. Chen, G. Coudurier, J.F. Joly and J.C. Vedrine, J. Catal., 143 (1993) 616.
[11] P. Nascimento, C. Akratopolou, M. Oszagyan, G. Coudurier, C. Travers, J.F. Joly and J.C. Vedrine, Stud. Surf. Sci. Catal., 75 (1993) 1185.
[12] C. Morterra, G. Cerrato, F. Pinna, M. Signoretto and G. Strukul, J. Catal., 149 (1994) 181.
[13] C. Morterra, G. Cerrato, C. Emanuel and V. Bolis, J. Catal., 142 (1993) 349.
[14] J.R. Sohn and H.W. Kim, J. Mol. Catal., 52 (1989) 361.
[15] S. Chokkaram, R. Srinivasan, D.R. Milburn and B.H. Davis, J. Coll. Int. Sci., 165 (1994) 160.
[16] D.A. Ward and E.I. Ko, J. Catal., 150 (1994) 18.
[17] G. Teufer, Acta Crystallogr., 15 (1962) 1187.
[18] F. Babou, B. Bigot and P. Sautet, J. Phys. Chem., 97 (1993) 11501.
[19] C. Li, P. Stair and W.M.H. Sachtler (private communication).
[20] V. Adeeva, G.D. Lei and W.M.H. Sachtler, Appl. Catal. A, 118 (1994) L11.
[21] M.R. Guisnet, Acc. Chem. Res., 23 (1990) 392.
[22] C. Bearez, F. Chevalier, M. Guisnet, Kinet. Catal. Lett., 22 (1983) 405.
[23] A.S. Zarkalis, C.-Y. Hsu and B.C. Gates, Catal. Lett., 29 (1994) 235.
[24] H. Liu, V. Adeeva, G.D. Lei and W.M.H. Sachtler, J. Mol. Catal., 100 (1995) 35.
[25] J. Tabora and R.J. Davis, J. Chem. Soc. Faraday Trans., 91 (1995) 1825.
[26] V. Adeeva, J.W. de Haan, J. Janchen, G.D. Lei, V. Schunemann, L.J.M. van de Ven, W.M.H. Sachtler and R.A. van Santen, J. Catal., 151 (1995) 364.
[27] C.H. Lin and C.Y. Hsu, J. Chem. Soc. Chem. Comm., (1992) 1479.
[28] M.A. Coelho, D.E. Resasco, E.C. Sikabwe and R.L. White, Catal. Lett., 32 (1995) 253.

[29] H. Liu, G.D. Lei, W.M.H. Sachtler, Appl. Catal. A, 146 (1996) 165.
[30] D.M. Brower, in R. Prins and G.C.A. Schuit (Editors), Chemistry and Chemical Engineering of Catalytic Processes, Sijthoff and Noordhof Publ., 1980, p. 145.
[31] T.K. Cheung, J.L. d'Itri and B.C. Gates, J. Catal., 153 (1995) 344.
[32] T.K. Cheung, J.L. d'Itri, F.C. Lange and B.C. Gates, Catal. Lett., 31 (1995) 153.
[33] C.Y. Hsu, C.R. Heimbush, C.T. Armes and B.C. Gates J. Chem. Soc. Chem. Comm., (1992) 1645.
[34] K.T. Wan, C.B. Khouw and M.E. Davis, J. Catal., 158 (1996) 311.
[35] E.C. Sikabwe, M.A. Coelho, R.L. White and D.E. Resasco, Catal. Lett., 34 (1995) 23.